2004-01-2017

Understanding the Relation Between Cetane Number and Combustion Bomb Ignition Delay Measurements

Andy D. B. Yates, Carl L. Viljoen and André Swarts
Sasol Advanced Fuels Laboratory, University of Cape Town

SAE *International*™

SAE ®

Global Mobility Database®

All SAE papers, standards, and selected books are abstracted and indexed in the Global Mobility Database.

For multiple print copies contact:

SAE Customer Service
Tel: 877-606-7323 (inside USA and Canada)
Tel: 724-776-4970 (outside USA)
Fax: 724-776-1615
Email: CustomerService@sae.org

Positions and opinions advanced in this paper are those of the author(s) and not necessarily those of SAE. The author is solely responsible for the content of the paper. A process is available by which discussions will be printed with the paper if it is published in SAE Transactions.

Persons wishing to submit papers to be considered for presentation or publication by SAE should send the manuscript or a 300 word abstract of a proposed manuscript to: Secretary, Engineering Meetings Board, SAE.

Printed in USA

Understanding the Relation Between Cetane Number and Combustion Bomb Ignition Delay Measurements

Andy D. B. Yates, Carl L. Viljoen and André Swarts
Sasol Advanced Fuels Laboratory, University of Cape Town

ABSTRACT

A recently approved method for cetane determination using the Ignition-Quality Tester (IQT™) is based on an ignition delay measurement in a combustion bomb apparatus, which is empirically correlated to cetane number. The correlation assumes that all fuels will respond to the different pressure and temperature domains of the IQT™ and the cetane test engine in the same way. This assumption was investigated at a more fundamental level by conducting IQT™ measurements at different pressure and temperature points and characterising the ignition delay of the fuel in terms of an Arrhenius autoignition model. The fuel model was combined with a mathematical model of the cetane engine and the concept was evaluated using a variety of test fuels, including the diesel cetane rating reference fuels. The analysis technique was able to accurately predict the cetane number in all cases.

INTRODUCTION

In a diesel engine, the propensity and timing of the fuel self-ignition event is a critically important factor that has implications for cold starting, engine noise, emission formation and power output. This attribute of a fuel is characterized by the cetane number which is a practical metric that is determined experimentally in a CFR test engine according to the ASTM D613 method [1]. The engine features a variable compression ratio and the method involves adjusting the compression ratio to obtain a predetermined time delay between the beginning of fuel injection and the first detectible pressure increase arising from combustion of the fuel. The cetane number is defined by the blending ratio of two primary reference fuels (n-cetane and heptamethyl nonane) that will produce the same ignition delay in the engine under the same operating conditions.

For the past fifteen years, a succession of SAE publications have described the development of an alternative method for determining the cetane number of a fuel [eg. 2,3,4]. The technique was based on a combustion bomb apparatus and was called the Ignition Quality Tester (IQT™). Its method of operation differed

from the ASTM D613 method in that the pressure and temperature of the combustion bomb were held constant and the ignition delay, as defined in the first paragraph, was measured. A calibration curve was determined empirically to provide the cross-reference between the measured ignition delay (ID) and the derived cetane number (DCN).

$$DCN = 83.99(ID - 1.512)^{-0.658} + 3.547 \quad \text{(eq. 1)}$$

The IQT™ apparatus and testing technique was approvd in June 2003 by the American Society for Testing and Materials (ASTM) as an alternative method for cetane number determination [5].

Whilst it has been demonstrated that the alternative method provides a measure of a fuel's cetane number over a limited range with acceptable accuracy, it is an acknowledged feature of the IQT™ device that the derived cetane number of blends of the primary reference fuels (PRF) and the secondary reference fuels (SRF) do not match each other, and neither are they aligned to their defined ASTM D613 cetane value [2,4]. Another quirk of the IQT™ device is that, when it is set up correctly, the ignition delay of the calibration reference fuel, n-heptane is 3.78 ms, which translates to a derived cetane number of 52.5. This is significantly different from the usual cetane number for n-heptane of 56 which is obtained by the ASTM D613 method [6].

These discrepancies seem to indicate that the correlation between the IQT™ ignition delay and the ASTM D613 cetane number cannot be accurately described for all fuels by a single calibration curve. This is a point that was clearly demonstrated by Siebers in 1985 [7] and the present paper attempts to investigate this issue by describing the autoignition behaviour of a test fuel in terms of a classical two-stage cool-flame autoignition model [8] combined with a single stage hot ignition. There are indications that this concept was also explored tentatively by Aradi and Ryan [2] but did not progress to full maturity. In theory, the proposed fuel characterisation could be evaluated for ignition delay under the IQT™ operating conditions as well as the CFR

engine operating conditions and could yield a more fundamental method for correlating the measured IQT™ ignition delay and the CFR engine compression ratio for any particular fuel. It was expected that the link between the CFR compression ratio and the fuel cetane number would approximately match the CFR guide curve and that the proposed analysis technique would effectively enable the direct determination of cetane number from IQT™ measurements without recourse to the use of a calibration formula.

MODELING APPROACH
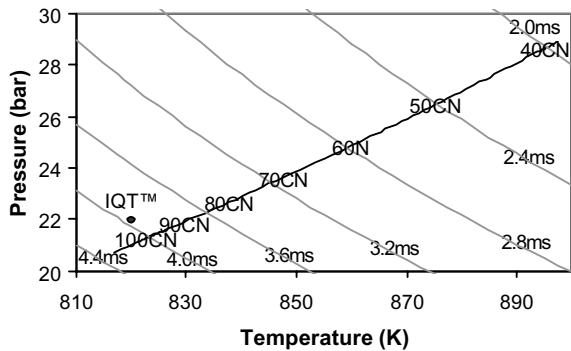
The above concept is illustrated in Figure 1.

Figure 1. The ignition delay contours for a 50 cetane fuel superimposed on the pressure-temperature domain for the CFR engine and the IQT™ apparatus

If a test fuel were subjected to an elevated pressure and temperature environment, it would exhibit a characteristic ignition delay before autoignition took place. This can be depicted as a contour plot in the pressure-temperature domain, as is depicted in Figure 1, which shows curves of constant ignition delay for a hypothetical fuel. The IQT™ test conditions correspond to a fixed point in the pressure-temperature domain and, with due regard for the fuel contours in this example, it is evident that the ignition delay for the test fuel in the IQT™ apparatus will be marginally under 4ms. In the CFR engine, the ASTM D613 cetane value is defined according to the compression ratio that will produce an ignition delay of 2.41 ms with the primary reference fuel blends. The peak pressure-temperature profile for the CFR engine is illustrated in Figure 1, with the relevant terminal points for different PRF cetane numbers labeled. For the test fuel in this example, the engine curve cuts the 2.41 ms contour at 50 CN, which implies that the test fuel has a 50 cetane rating.

The hypothetical case of a different test fuel is illustrated in Figure 2. Whilst the ignition delay at the pressure and temperature corresponding to the CFR engine 50 CN point is also 2.41 ms, which would define the fuel as also having a 50 cetane rating, the ignition delay contours would not necessarily be identical to the first test fuel. As a result, the ignition delay measured at the IQT™ point could be different from that of the first test fuel and the

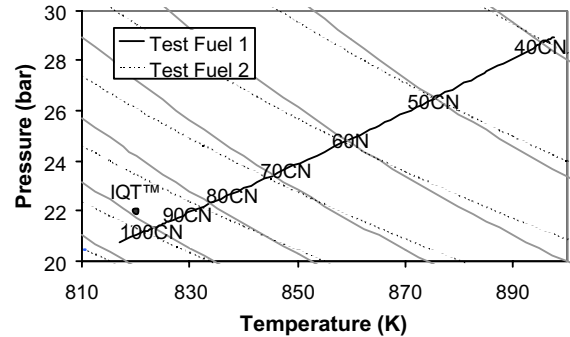derived IQT™ cetane numbers for the two test fuels would differ.

Figure 2. A second, different test fuel, also having a cetane rating of 50, illustrated by the dashed contour lines

AUTOIGNITION CHARACTERISATION

Considerable study and speculation has been devoted to determining the causal relationship between the molecular structure of a fuel and its spontaneous combustion behaviour. At present, the chemical kinetic descriptions of the complex oxidation reactions are not sufficiently well developed to enable a completely predictive mathematical model to replace the experimental test method, although the gap between model and experiment is closing steadily.

Various approaches to the modeling of autoignition characteristics of both spark ignition and compression ignition fuels are possible; ranging from a completely global, single-step description [9], to a reduced kinetics treatment [10,11,12,13], or a comprehensive, detailed chemical kinetic simulation [14]. A single, global reaction approach attempts to represent the sum of all hydrocarbon oxidation reactions leading to autoignition, by a single Arrhenius equation, having a rate constant, k_G of :

$$k_G = A_G \; e^{(\frac{-Ea}{RT})}$$

where the subscript, G, refers to the global reaction, A_G is the pre-exponential constant of proportionality and E_a is the activation energy for the global reaction. For zero order and first order reactions

$$\tau_G = \frac{Const}{k_G}$$

where τ_G is the mean lifetime of all the reactant molecules. For first order reactions, the constant is unity [15]. If one makes allowance for a possible pressure dependence in the global reaction, as indicated by early experiments [16], the well known ignition delay

relationship which was used to good effect by Livengood and Wu [17] and Douaud et al [18] is obtained:

$$\tau_G = A_G \ \ p^{-n_G} e^{(\frac{B_G}{T})}$$

From the earliest experimental results obtained by rapidly compressing fuel-air mixtures and studying the cool flame evolvement, it was clear that the summation of two different ignition delays were required to describe the data in the low and intermediate temperature regions where these measurements had been made [8,16]. Edwards et al. [19] identified the temperature range below 700 K as "low", from 700 - 1100 K as being "intermediate", and >1100 K as the "high" temperature regime. More recently however, most workers in the field of detailed kinetics of hydrocarbon oxidation, prefer not to distinguish a separate low temperature regime, but rather to identify the range from 600 - 900 K as the low-intermediate-temperature regime [20]. The high temperature region is then mostly defined as > 900 K.

The development and validation of comprehensive detailed reaction mechanisms for hydrocarbon oxidation over the last decade by especially Curran, Pitz and Westbrook [21,22], have shown that the high temperature ignition can be adequately described by 9 elementary classes of reactions, e.g. unimolecular fuel decomposition, H atom abstraction to form an alkyl radical, alkyl radical decomposition, etcetera. The low and intermediate temperature mechanism is significantly more complex and a further 16 classes of elementary reactions are needed, starting with the addition of molecular oxygen to an alkyl radical: $R\bullet + O_2 <=> RO_2\bullet$ followed by internal H atom abstraction, a second addition of O_2, another H atom abstraction and subsequent decomposition of the ketohydroperoxide species to yield 2 reactive hydroxyl radicals and a carbonyl radical. This sequence, producing 3 radicals from one fuel radical, is responsible for the low temperature chain-branching process.

DETAILED KINETIC MECHANISM FOR n-HEPTANE

Although a discussion of the detailed mechanism of Curran et al. [21] for n-heptane, consisting of 2450 elementary reactions among 550 chemical species, falls outside the scope of this article, it must be noted that this elaborate mechanism also models the two-stage cool flame ignition and the subsequent hot ignition very well. Similarly, most reduced mechanisms such as the Shell model [10], the Cox and Cole mechanism [12], and subsequent Hu and Keck [23] schemes have been "designed" to describe the three stage behaviour of hydrocarbon oxidation. Griffiths [24] pointed out, however, that these reduced models still fail to describe the transition to high temperature reactions, above approximately 1200 K, in a satisfactory manner.

Typical examples of experimental shock tube data are shown in Figure 3. These indicate the principal features of the cool flame ignition delay region, the intermediate region of negative temperature coefficient (NTC) behaviour and the high temperature ignition region.
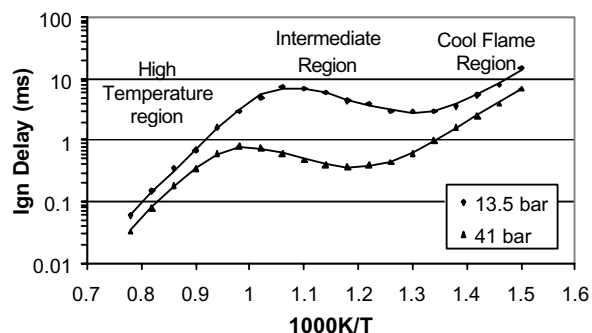

Figure 3. The proposed Ignition-delay model fitted to data extracted from Tao et al [25] for n-heptane

The cool flame ignition delay (τ_1) is largely associated with the decomposition, at a temperature between 800 and 850 K, of the ketohydroxide species that had gradually been building up in the system, leading to rapid chain branching and sudden heat release.

In the low-intermediate temperature region (< 900 K), the most important reactions for alkyl radicals $R\bullet$ are additions to molecular oxygen: $R\bullet + O_2 <=> RO_2\bullet$ (where $RO_2\bullet$ is an alkylperoxy species). The activation energy for the addition reaction is taken to be zero, but in the reverse (dissociation) direction it is quite large at ˜ 30 kcal/mol [21]. Thus the equilibrium constant for this reaction is very strongly temperature dependent. At very low temperatures this reaction proceeds rapidly to alkylperoxy species, whilst at high temperatures $RO_2\bullet$ dissociates rapidly back to its reactants and the concentration of $RO_2\bullet$ becomes very small, effectively shutting off the low temperature branching reaction paths at approximately 900 K. This has the effect of also lowering the overall rate of reaction and accompanied heat release [26].

Pressure also influences the $R\bullet + O_2 <=> RO_2\bullet$ equilibrium through the well known Le Chatelier principle. At elevated pressures, the $RO_2\bullet$ submechanisms continue to be important at higher temperatures than would have been the case for a system at atmospheric pressure [22]. During rapid compression machine studies of n-pentane, Westbrook observed that a pressure increase by a factor of x 2 increased the temperature where decomposition begins to control the reaction by 50°C [26]. The region of minimum heat release (NTC) also shifted 50°C towards a higher temperature. Thus the complex NTC behaviour is determined by the $RO_2\bullet$ equilibrium described above, rather than by a single reaction. In the present paper we associate this $R\bullet + O_2 <=> RO_2\bullet$ equilibrium with τ_2.

Finally, the high temperature ignition at temperatures above 900 K is driven primarily by the decomposition of hydrogen peroxide. If the temperature of the system has advanced beyond the region of negative temperature coefficient, then a positive temperature dependence of ignition delay on temperature is again observed. The activation energy for H_2O_2 decomposition is large enough (~45 kcal/mol) [26] so that its decomposition is still quite slow in the range from 800 K to 1000 K. Above 1000 K, rapid decomposition of H_2O_2 and the associated hot ignition is observed.

At these high temperatures, alkyl radical decomposition through ß-scission, as well as direct unimolecular fuel decomposition [21] becomes feasible alternative paths leading to hot ignition. However, for the purposes of this paper we associate the third ignition delay, τ_3, only with the H_2O_2 decomposition reaction leading to rapid chain branching through the production of two reactive OH• radicals from every H_2O_2 molecule [26].

MATHEMATICAL MODEL OF AUTOIGNITION

The current objective was to describe the complex kinetic chemistry of hydrocarbon autoignition in the simplest mathematical formulation that could be shown to be consistent with the available experimental and literature data. Thus, the proposed model involved two distinct regimes; a two-stage, low-temperature regime and a single stage high temperature regime. The ignition delays for each stage were described by a general Arrhenius function:

$$\tau_i = A_i p^{n_i} e^{\frac{B_i}{T}} \qquad \text{(eq. 2)}$$

Since the two stages of the low-temperature regime were sequential, they were expressed as the arithmetic sum of the individual ignition delays, $\tau_1 + \tau_2$. Since the high, temperature delay, τ_3 represented an alternative, competing pathway, the overall ignition delay for the full temperature spectrum was described by the sum of the individual rates, ie, the inverse sum of the two delays:

$$\tau_{overall} = \left\{ (\tau_1 + \tau_2)^{-1} + (\tau_3)^{-1} \right\}^{-1} \qquad \text{(eq. 3)}$$

EVALUATION AGAINST LITERATURE DATA

The model was tested against data that was extracted from the literature to determine the typical ranges for the coefficients A_i, n_i and B_i for each of the three stages 1, 2 and 3.

Figure 3, which was referred to earlier, shows the results of a least-squares fit of the ignition delay model to the data presented by Tao et al [25]. A wide temperature range was covered and the data encompassed two pressure values which enabled all nine coefficients to be

determined, as listed in Table 1. The coefficient values for τ_1 and τ_2 were found to be similar in magnitude to typical values quoted by Lewis and von Elbe [3] and others.

Table 1. The ignition delay model coefficients used to generate the trend-lines shown in Figure 3

	Ln (A_i)	n_i	B_i
Stage 1	-15.3	-0.580	12900
Stage 2	17.2	-2.60	-7550
Stage 3	-17.4	-0.506	20400

A similar analysis was carried out with data published by Hoskin et al [27]. This data was particularly relevant because it included PRF blends and was conducted in a combustion bomb apparatus. The data set was limited to only one pressure and therefore the values for the pressure coefficients, n_i, listed in Table 1 were used. Also, the range of temperatures that were investigated by Hoskin et al did not extend fully into the high-temperature regime and there was insufficient data to determine A_3 and B_3 independently. The value of B_3 from Table 1, which represents the slope of the high-temperature regime, was therefore retained and the value of A_3 was calculated. The results of the regression analysis are depicted in Figure 4 and the corresponding fuel-specific coefficients are listed in Table 2. Significantly, it was found that an acceptable fit to the data could be obtained with a single value for the coefficients A_1, B_1 and A_2, with adequate differentiation between the PRF blends being encapsulated by varying B_2 only.

As can be seen from Figure 4 the optimal value of B_2, which is reflected in the gradient in the intermediate region, was positive. This indicated that the second stage ignition was not exhibiting a fully negative temperature sensitivity in the combustion bomb.
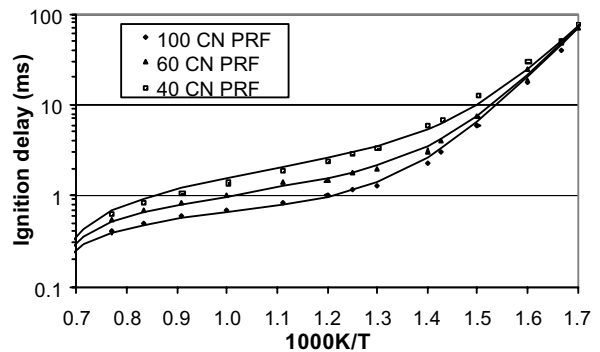

Figure 4. The proposed ignition-delay model fitted to data extracted from Hoskin et al for PRF blends at a pressure of 13.5 bar [27]

Table 2. The ignition delay model coefficients used to generate the trend lines shown in Figure 3

	40 CN PRF	60 CN PRF	100 CN PRF
$Ln(A_1)$	-15.8		
$Ln(A_2)$	6.87		
B_2	2400	1960	1540
$Ln(A_3)$	-12.9		
** All other coefficients as for Table 1			

Similar curves are also shown in other references [6, 19], indicating that constant volume combustion bombs may cause the negative temperature coefficient behaviour to be less pronounced than for the same fuel in a shock tube. One possible reason for this is the different time-scales involved in a shock tube (effectively instantaneous pressure increase, so that the end gas is not exposed to a pressure-temperature history), compared to combustion bombs and rapid-compression machines (RCM). Westbrook et al have noted that significant fuel conversion, and heat release, may already take place during the compression phase in a RCM, leading to less pronounced NTC behaviour than is observed in a shock tube experiment [28].

Consideration was given to the possibility that the physical processes associated with the fuel injection would cause a lack of homogeneity – both in terms of fuel and temperature distribution, and this may have been responsible for lack of apparent NTC behaviour. Warnatz et al [29] describe the results of a detailed examination into the combustion of droplets and sprays, subdividing the event into a heating phase, an evaporation phase and a combustion phase. They used methanol for their study since it had a relatively high latent heat of evaporation which accentuated the physical processes. Their study over a range of temperatures indicated that the ignition delay times increased by factor of x 2 when the fuel droplet diameters were increased by a factor of x 10. The significant point here was that the fuel evaporation could be adequately represented as a scaling factor, which meant that it could be effectively accommodated by the A_i coefficients in terms of the proposed model.

ENGINE MODEL

A two-zone engine model was used to represent the divided-chamber attributes of the CFR cetane engine. Attention was given to the losses associated with the inter-leading passage between the main cylinder chamber and the combustion chamber which featured the expansion plug for adjusting the compression ratio. Unlike modern-day pre-chamber diesel engines, the size of the CFR engine throat was relatively large and did not pose a significant restriction between the two chambers at the low speed (900 rpm) at which the engine was operated.
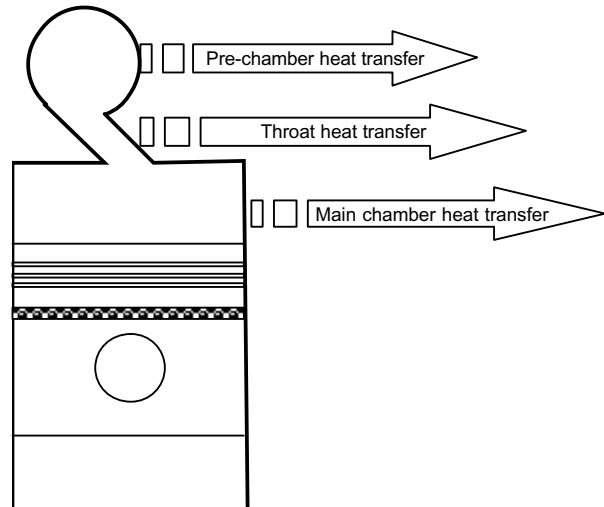

Figure 5. Illustration of the different heat transfer zones applied to the engine model

The model was constructed such that the two chambers shared a common pressure and bulk heat transfer was solved in three distinct zones; the pre-chamber, the throat and the main chamber. These are illustrated in Figure 5.

The cylinder heat transfer was calculated following the model by Woshni [30], but parameters were optimised for the CFR engine geometry. The heat transfer in the pre-chamber considered the geometrical changes associated with changing the expansion plug position, whilst heat transfer coefficients in the pre-chamber and throat was based on steady forced convection at the expected flow velocities. The temperature of the cylinder wall was based on experience and measurements on the CFR octane engine, whilst the throat and pre-chamber wall temperatures were optimised to match with the expected compression pressures.

Although the combustion event was not included in the model, typical values for the residual exhaust gas were used in the calculation of the initial trapped gas temperature and gas composition.

The gas temperatures of the individual chambers were found by applying two energy balances during the engine cycle. The overall energy balance included the total mass, total work done and total heat losses, whereas the second energy balance considered only the pre-chamber. Throat heat transfer as well as mass and energy exchange with the main-chamber was included. The pressure and temperature profiles that were thus generated were used as input parameters for the ignition delay model. The compression ratio was determined iteratively to obtain an ignition delay of 2.41 ms, which is the defined set-point for cetane determination according to the ASTM D613 method [1].

It is self evident that, in the final stage of the analysis, there must be an empirical correlation between cetane number and compression ratio in the engine. This is equally true for both the CFR engine and mathematical engine model. In the case of the CFR engine, this guide curve is defined by the primary reference fuels and it follows that the guide curve for the mathematical model should be defined in the same way, ie, using the primary reference fuels. In order to compare the model guide curves with the CFR engine, the relationship between cetane number and compression ratio for the physical CFR engine was sought, and the acquisition of this information proved to be more of a challenge than one would have expected.

THE CETANE GUIDE CURVE

The ASTM D613 manual acknowledges that there is a correlation between cetane number and compression ratio. However, unlike the octane methods, it does not currently provide a guide curve [1].

The CFR engine compression ratio is adjusted by means of a hand-wheel which is integrated with a micrometer scale. For several decades, the ASTM manual contained a formula which linked the compression ratio to the hand-wheel micrometer reading:

$$Comp\ Ratio = \frac{18 + handwheel\ reading}{handwheel\ reading}$$ (eq. 4)

The 1948 issue of the ASTM D613 manual prescribed a volume calibration procedure for establishing the set-point for the hand-wheel reading [31]. The specification called for a predefined volume of water to fill the clearance volume when the hand-wheel micrometer was set to 2" (corresponding to a compression ratio of 10). The quoted clearance volume at this point was 68 ml (4.15 cu. in.). A curve relating cetane number to hand-wheel measurement was also provided in this issue of the manual. From this information, it was possible to construct the guide curve that is shown in Figure 6.

In later issues of the ASTM D613 manual [32], the volumetric method for calibrating the micrometer set-point was replaced by a compression pressure test procedure. This stipulated a compression pressure of 32.3 ± 1.4 bar (gauge) for a fully warmed engine operating at 900 r/min with the hand-wheel set at 1". The equation relating the compression ratio to the hand-wheel reading remained unchanged, which implied that the pressure test was conducted at a theoretical compression ratio of 19. A simple polytropic compression calculation, using typical values, indicates that the compression ratio and the compression pressure are, however, irreconcilable. This glaring discrepancy was not addressed in the ASTM manual for several decades.

In the 1995 CFR engine operator's handbook [33] it was noted that "*The D 613 table, which appeared in the*

standard, was apparently calculated without taking into account the turbulence passage, pickup passage, and combustion chamber volumes." The information supplied in the handbook indicated that the compression test was in fact being conducted at a compression ratio of 16.5 rather than 19. Besides resolving the compression pressure inconsistency, this implied that the hand-wheel setting was effectively shifted by 0.162" from the originally defined calibration point. The 1995 CFR engine handbook also included a typical curve depicting the relationship between cetane number and hand-wheel reading. Since the curve was very similar to the 1948 ASTM data, it was apparently based on the original micrometer scale setting. This was confusing since one might have expected the authors of the handbook to have expressed the cetane curve in terms of the more recent hand-wheel calibration. This guide curve is also shown in Figure 6, with the handwheel readings converted to compression ratio using equation 4.

It is interesting to note in passing that the latest version of the ASTM D613 manual does not mention the error contained in the earlier issues. Whilst the compression pressure calibration procedure has been retained, all the pertinent information that would enable the determination of the compression ratio in terms of the hand wheel micrometer setting has been removed.
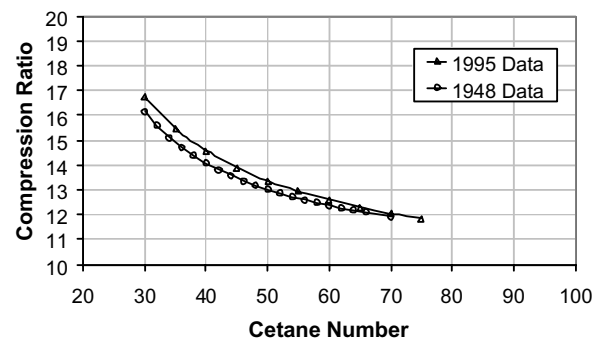

Figure 6. Guide curve relating the compression ratio to cetane number based on the ASTM D613 manuals

EXPERIMENTAL TESTS

In order to fully characterise a fuel in terms of its response to pressure and temperature, it would be necessary to conduct a series of measurements over a wide range of different pressures and temperatures corresponding to those typically encountered in the CFR engine. As indicated in Figure 1, however, the engine regime was typically well beyond the operating pressure and temperature for the IQT™ apparatus and to conduct tests in this regime would have exceeded the safe operating limits. The pragmatic solution was to conduct ignition-delay measurements at reduced pressures and temperatures and to extrapolate the fuel behaviour with the aid of a fuel model.

IQT™ TESTS

The tests were conducted in strict accordance with the equipment operating guidelines. Daily checks were carried out to verify the combustion bomb sealing integrity. The various calibrations procedures were carried out routinely and a n-heptane reference test was conducted at the start and end of each session.

Experience with the apparatus indicated that it was helpful to use multiple compressed air cylinders in order to extend the cylinder change intervals and the associated recalibration. Problems were initially experienced with the exhaust valve sealing and, since the bomb was being used for research rather than production testing, a small design improvement was implemented that solved the problem permanently.

A sensitivity analysis revealed that the precision of the IQT measurement was extremely important to the precision of the overall cetane analysis. This is illustrated in Figure 7, which depicts the extrapolation required for a 50 cetane fuel in the temperature domain. (A similar argument would apply for the extrapolation in the pressure domain.) The diagram illustrates that the uncertainty in the ignition delay at the CFR engine point can be improved by increasing the separation between the IQT reference point and the reduced temperature (or pressure) measurement point. A separation of -50°C was selected for the temperature domain and -9 bar in the pressure domain. Alternatively, the overall precision could be improved by reducing the uncertainty of the measured IQT ignition delay. The precision of the IQT reference point is more important in this regard since it is closer to the engine operating point. For this research investigation, a minimum of three measurements were made at the reference point an in many instances, particularly in the case of n-heptane and the PRF blends, several additional measurements were made.
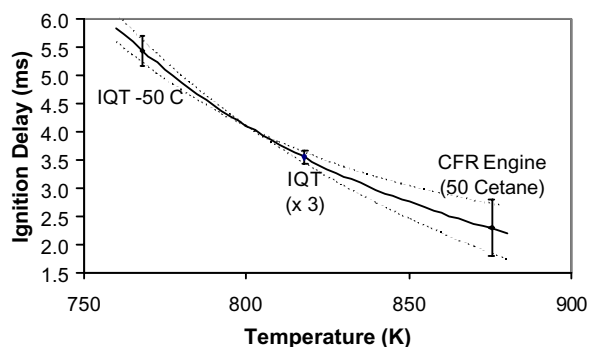

Figure 7. Illustrating the influence of measurement precision and the sensitivity to temperature extrapolation. (Values increased for illustration.)

Combustion bomb measurements taken at three different operating points were reported by Aradi and Ryan for a variety of diesel fuels [2]. Ideally, for the purposes of the present analysis, the pressure and temperature should be varied orthogonally to avoid a possible autocorrelation error. However, because the authors were attempting to simulate a constant-density situation, this precaution was not applicable and the pressure and temperature variations were synchronised. Despite this caveat, their data was included and evaluated using the proposed analysis technique since it represented a valuable additional means to testing the robustness of the method.

TEST FUELS

The Primary Reference Fuels (PRFs) for cetane number determination according to ASTM D613 [1] are n-hexadecane (n-cetane), having a cetane rating of 100.0, and 2,2,4,4,6,8,8-heptamethyl nonane (HMN), having a cetane rating of 15.0. Volumetric blends of these 2 pure components (sourced from Humphrey Chemical Company) were made with a high precision electronic burette, under constant temperature conditions, to obtain the required PRF standards of 40.0, 50.0, 60.0, 80.0 and 100.0 cetane number.

In a similar fashion, the secondary cetane standards (obtained from Chevron Phillips Chemical Company) were used to make the Secondary Reference Fuels (SRFs). Blends were made with the U-15 lower cetane standard (18.7 CN) and the T-22 higher cetane standard (74.8 CN), according to the blend ratio instructions supplied by Chevron Phillips. The standard 400 ml glass burettes were used to obtain the 40.0, 50.1, 55.1, 60.2 and 74.8 SRFs.

n-Heptane, specified as the calibration fuel for the IQT™ apparatus [5], was included as a test fuel. As indicated in the introduction, n-heptane has a D613 cetane rating of 56.0 [6]. Finally, a matrix of 3 full-boiling range market diesels was also added to the investigation, to span the range of cetane numbers of interest, from 40 to 75. These were a low cetane 2D diesel, imported from the USA, a local ultra-low sulphur synthetic diesel produced by Sasol, named Turbodiesel™, and a Sasol SPD™ diesel sample obtained from the Sasol Slurry Phase Distillate Process. The ASTM D613 cetane numbers of the 3 fuels are shown in Table 3.

Table 3. Cetane Numbers for the full-boiling range diesels used in this study

Diesel Fuel	ASTM D613 Cetane Number
US -2D	40.3
Sasol Turbodiesel™	56.4
Sasol SPD™ diesel	75.4

Finally, the relevant fuel data that was extracted from reference 2 is listed in Table 4. This represented a typical full-boiling range fuel, blended with two types of cetane improver additive. A three-component model fuel was also listed which represented the three major constituents found in normal diesel fuel.

Table 4. Fuel data extracted from Reference 2

Diesel Fuel	ASTM D613 Cetane Number
* US 2D (28.8% aromatics)	46.5
* US 2D + 2EHN (0.25%)	52.5
* US 2D + DTBPO (0.25%)	49.7
* US 2D + Mix (0.125% 2EHN and 0.125% DTBPO)	49.9
* 3-Part Model (35% n-cetane, 35% 1-methyl naphthalene, 30% decalin)	46.6

RESULTS AND DISCUSSION

The application of the ignition delay model to the literature data has clearly revealed that certain of the fuel coefficients could be treated as quasi constant. Based on these observations, the following assumptions were made for the analysis of the PRF blends:

- Coefficients for stage 1 and stage 3 ignition delay were set to approximately the same values as were computed for the Hoskin et al PRF data (see Table 2) and then optimized for the minimum least-squares error.

- Coefficients for stage 2 were computed, but the A_2 coefficient was constrained to a single value for all the blends, as was found to be sufficient for the Hoskin et al data (see Table 2).

Since there were several repeated ignition delay measurements available for each fuel, the solution was over-determined and a least-squares regression technique was used to determine the best-fit values for the variable fuel coefficients. Despite the multiple measurements at particular pressure and temperature points, there were essentially only three degrees of freedom reflected in the data (three basic operating points). The effect of constraining one of the variables to a single value for all the blends was did not have a negative influence on the overall correlation coefficient, which suggested that this was a valid underlying fuel characteristic as was also proposed in Table 2.

The results of the analysis are illustrated in Figure 8 and the fuel coefficients are summarized in Table 5. The standard deviation in the error of the calculated ignition delays for the five PRF blends was 0.04 ms, which

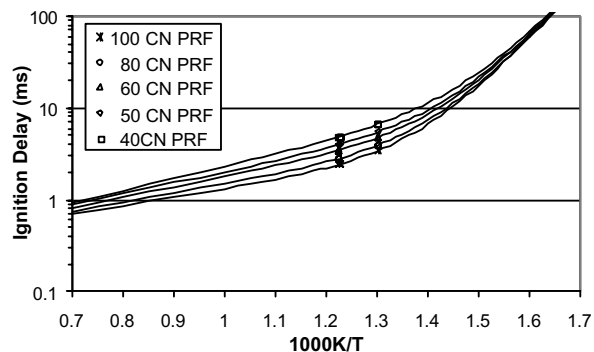compared favorably with the typical standard deviation of 0.081 ms resulting from a single IQT™ measurement.

Figure 8. The ignition delay model for PRF blends based on the IQT measurements at two temperature points. (Pressure = 22.2 bar)

Table 5. Fuel coefficients for the PRF blends

	40 CN PRF	50 CN PRF	60 CN PRF	80 CN PRF	100CN PRF
$Ln(A_1)$	-16.4 (optimized ≈ Table 2)				
n_1	-0.5 (optimized ≈ Table 1 & 2)				
B_1	13 480 (optimised ≈ Table 1 & 2)				
$Ln(A_2)$	1.21				
n_2	-1.087	-1.035	-1.028	-0.993	-0.974
B_2	2994	2690	2550	2264	2078
$Ln(A_3)$	-8.75 (optimized ~ Table 2)				
n_3	-0.506 (= Table 1 & 2)				
B_3	20430 (= Table 1 & 2)				

The derived fuel PRF coefficients were used in conjunction with the engine model to infer the compression ratio at which the prescribed 2.41 ms ignition delay would occur with each blend. The resulting "virtual" guide curve is shown in Figure 9, together with the ASTM typical guide curve that was depicted in Figure 6. The general correlation with the ASTM guide curve was regarded as encouraging validation of the proposed technique
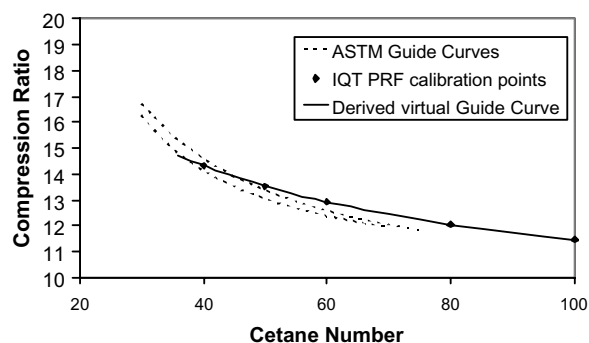.

Figure 9. The derived "virtual" guide curve based on the ignition delay data for PRF blends.

The technique was used to evaluate the derived cetane rating of the five SRF blends and n-heptane. In this case, each fuel was treated in isolation. The fuel coefficients were calculated according to the following strategy:

- The coefficients for stage 1 and stage 3 were set to the same value as was used for the PRF analysis.
- The three coefficients for stage 2 were treated as variables and were computed using the least-squares regression.

The fuels were evaluated using the engine model and the compression ratio was determined iteratively to yield an engine ignition delay of 2.41 ms as before. The derived cetane number was then inferred from the PRF "virtual" guide curve shown in Figure 9. The resulting match between the derived cetane number and the ASTM D613 cetane numbers is shown in Figure 10. The numerical results are given in the Appendix.

The standard deviation of the error in the derived cetane number was 0.74 CN, which is approximately equal to the repeatability of the D613 method. As might be expected, the PRF fuels correlated extremely well with the D613 cetane number since they were used for the determination of the guide curve. However, a significant advantage of the analysis technique was recognized inasmuch that it circumvents the problem of the reproducibility of the CFR test engine. Also, the calibration with the PRF blends need only be done once and there is obviously no requirement to bracket each test fuel as is stipulated for the D613 test procedure.

For comparison, the derived cetane correlation using the IQT™ empirical formula is depicted in Figure 11. Whilst the correlation in the ASTM approved range of 40 DCN to 56 DCN [5] is reasonable, it is clear that the present proposed technique provides a considerably improved cetane prediction at the higher values, up to 100 cetane.
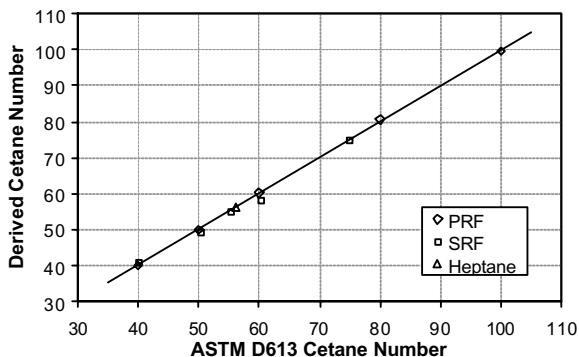

Figure 10. The derived cetane prediction for the PRF and SRF blends and n-heptane
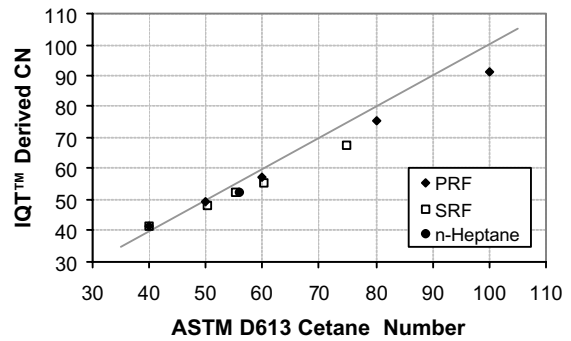

Figure 11. The IQT™ derived cetane number for the PRF and SRF blends and n-heptane, based on equation 1.

DISCUSSION REGARDING HEPTANE AND FUEL DIFFERENTIATION

Although its carbon number is considerably different from typical diesel fuels, n-heptane has been widely studied and modelled. It also has a special significance because it is the reference fuel for calibrating the IQT™ apparatus. A series of additional ignition delay measurements was performed with this fuel at reduced temperatures ranging from T_{ref} - 50°C to T_{ref} - 180°C, and the results are shown in Figure 12.
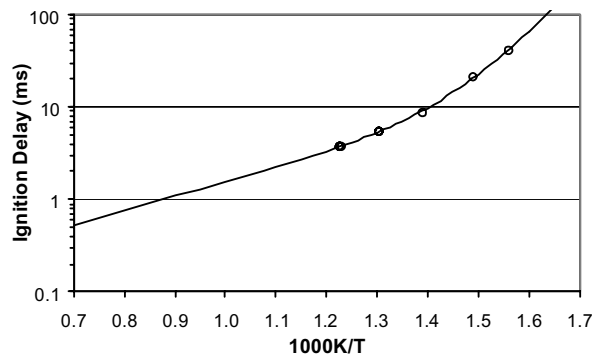

Figure 12. Additional data points for n-heptane measured in the temperature domain (Pressure = 22.2 bar).

It was seen form Figure 12 that the ignition delay model was clearly providing an appropriate degree of flexibility to match the measured ignition delay profile of the fuel. Because of the additional number of data points, the confidence in the calculated model coefficients was enhanced, and it was found that derived cetane value was 56.0, which matched the reported cetane value exactly [6].

In the introduction to this paper, it was postulated that the discrepancies encountered with the IQT™ calibration curve (equation 1) could be related to fuel-specific variations in the sensitivity to pressure and temperature.

This is clearly shown by the values of the calculated n_2 and B_2 coefficients which are illustrated in Figure 13 for the PRF and SRF blends. Apart from the trends exhibited within the individual blends which is interesting in itself, a clear differentiation between the PRF and SFR blends was revealed. This clearly indicated that their ignition delay responses would be irreconcilable in terms of a single calibration curve as is embodied in the IQT™ calibration curve.

The coefficients for n-heptane, also shown in figure 13, emphasise its segregation from normal diesel fuel behaviour. If the proposed analysis technique were to be used to describe alternative fuels such as DME, biodiesel, alcohol fuels, etc, it would be recommended to conduct several ignition delay measurements over a wider range of pressures and temperatures to enable the coefficients for the ignition delay to be determined with confidence.
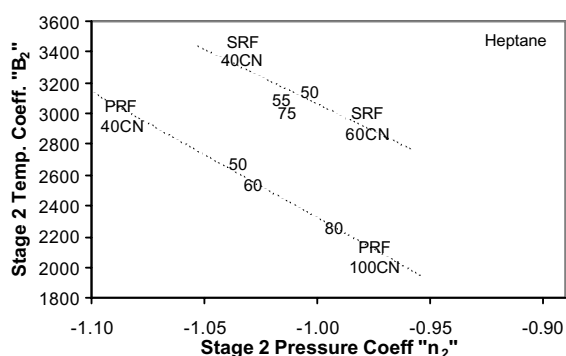
Figure 13. Illustration of the pressure and temperature coefficient grouping

FULL BOILING RANGE FUELS

The analysis strategy that was used for the SRF blends was similarly applied to the full boiling range fuels. This worked well for the fuels listed in Table 4, but the least squares error for the five fuels listed in Table 4 indicated a very poor regression fit. The ignition delay data for these fuels had been extracted from published literature and represented typical market fuels that contained aromatics and cetane additives. A variance analysis indicated that the three most significant variables for these fuels were A_2, B_2 and A_3. A median value of $n_2 = 0.6$ was therefore used and the analysis variables for these fuels were changed appropriately.

The result of the cetane number determination is shown in Figure 14. An uncertainty band corresponding to a total spread of 3.6 cetane numbers (approximately reflecting the ASTM defined reproducibility) was ascribed to the D613 cetane ratings for these fuels since they were based on actual measurement, as opposed to the reference fuels for which the cetane number was defined exactly. The overall predictive capability of the proposed technique was clearly demonstrated over the cetane range from 40 CN to 75 CN. It was particularly gratifying to see that the technique worked well for the fuels to which a cetane improver had been added. As with the PRF and SRF blends, the calculated model coefficients for each fuel were quite distinct and each fuel was uniquely characterised which enabled a successful and accurate transition from the combustion bomb conditions to the engine operating conditions in terms of pressure and temperature.
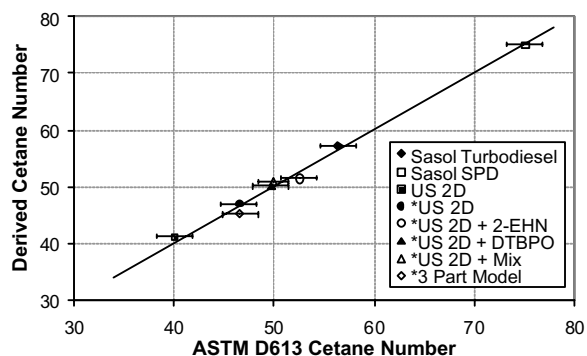
Figure 14. Prediction results for the full-boiling range fuels, based on measured IQT data and published data, and including fuels dosed with cetane-improving additives.

CONCLUSIONS

An improved method of deriving the D613 cetane rating from ignition delay measurements in a combustion bomb has been investigated. By using a flexible fuel auto-ignition model that was founded on well established chemical principles, the technique was able to accurately describe a fuel's ignition delay response to changes in pressure and temperature. This, in itself is useful information. When it was coupled with a comprehensive model of the CFR cetane engine, the technique provided a means for accurately determining the cetane number. The standard deviation of the error in cetane prediction was better than 0.8 CN for all the fuels that were evaluated. In terms of empirical calibration relationships, the proposed method was reliant only on the correlation between cetane number and compression ratio that is also an intrinsic feature of the D613 method.

The analytical results were able to explain the root cause for inconsistencies in the IQT™ derived cetane numbers when applied to PRF and SRF blends. The conflict regarding the nonconforming IQT™ derived cetane value for n-heptane of 52.5 CN was also addressed by the proposed analysis technique which agreed exactly with the commonly reported D613 cetane rating of 56 CN for n-heptane.

The selection of the most appropriate fuel coefficient variables to describe the ignition delay is an area for further research and investigation, as is the choice of appropriate values for the coefficients that are not directly calculable from the regression analysis. The next step in the evaluation of the proposed technique would be a more comprehensive and fundamental investigation into the effect of fuel compositional variations in terms of the three ignition delay phases that have been identified.

It is also clear that the methodology of quantifying the ignition delay of a fuel in terms of a simple response to the applied pressure and temperature is a powerful technique that could be usefully employed in other auto-ignition applications such as the study of HCCI and CAI combustion and octane rating.

ACKNOWLEDGEMENTS

REFERENCES

1. ASTM Method D613-03b, "Standard Test Method for Cetane Number of Diesel Fuel Oil", ASTM, August 2003
2. Araldi A. A., Ryan III T. W., "Cetane Effect on Diesel Ignition Delay Times Measured in a Constant Volume Combustion Apparatus", SAE 952352, 1995
3. Allard L. N., Webster G. D., Hole N. J., Ryan T. W., Ott D., Fairbridge C. W., "Diesel Fuel Ignition Quality As Determined In The Ignition Quality Tester (IQT)", SAE 961182, 1996
4. Allard L. N., Webster G. D., Hole N. J., Ryan T. W., Bker G., Beregszaszy A., Fairbridge C. W., Ecker A., Rath J., "Analysis Of The Ignition Behaviour Of The ASTM D-613 Primary Reference Fuels And Full Boiling Range Diesel Fuels In The Ignition Quality Tester (IQT™)—Part III", SAE 1999-01-3591, 1999
5. ASTM Method D6890-03, "Standard Test Method for Determination of Ignition Delay and Derived Cetane Number (DCN) of Diesel Fuel Oils by Combustion in a Constant Volume Chamber", ASTM, August 2003
6. Rose J. W., Cooper J. R., "Technical Data on Fuel", 7th ed, Scottish Academic Press, 1977
7. Siebers, D.L., "Ignition Delay Characteristics of Alternative Diesel Fuels: Implications on Cetane Number", SAE 852102, (1985)
8. Lewis B., von Elbe G., "Combustion, Flames and Explosions of Gases", 2nd ed, Academic Press, 1961
9. Warnatz, J., "Hydrocarbon oxidation high-temperature chemistry", Pure Appl. Chem., Vol.72, No.11, p. 2101, 2000.
10. Halstead, M. P., Kirsch, L. J., and Quinn, C. P., "The Autoignition of Hydrocarbon Fuels at High Temperatures and Pressures –Fitting of a Mathematical Model", Combustion and Flame 30, 45-60 (1977)
11. Kirsch, L. J., and Quinn, C. P., "A fundamentally based model of knock in the gasoline engine.", Sixteenth Symposium (Int.) on Combustion, The Combustion Institute, p.233-244, (1976)
12. Cox, R.A., and Cole, J.A., "Chemical aspects of the autoignition of hydrocarbon-air mixtures.",Comb and Flame, 60, p.109-123 (1985)
13. Schreiber, M., Sadat Sakak, A., Lingens, A, and Griffiths, J.F., "A reduced thermokinetic model for the autoignition of fuels with variable octane ratings.", Twenty-fifth Symposium (Int.) on Combustion, The Combustion Institute, p.933-940, (1994)
14. Westbrook, C.K., Warnatz, J., and Pitz, W.J., "A detailed chemical kinetic reaction mechanism for the oxidation of iso-octane and n-heptane over an extended temperature range and its application to analysis of engine knock.", Twenty-second Symposium (Int.) on Combustion, The Combustion Institute, p.893-901, (1988)
15. Logan, S.R., "Fundamentals of Chemical Kinetics", Longman, p 10, (1996).
16. Fish, A., Read, A., Affleck.W.S., and Haskell, W.W, "The controlling role of cool flames in two-stage ignition.", Combustion and Flame, Vol. 13, p.39-49, (1969)
17. Livengood, J. C., Wu, P. C., "Correlation Of Autoignition Phenomena In Internal Combustion Engines And Rapid Compression Machines", 5th Symp. (Int.) on Combustion, p. 347, Reinhold Publishing Corp. (1955).
18. Douaud, A. M., Eyzat P., "Four Octane Number Method for Predicting the Anti-Knock Behaviour of Fuels and Engines" SAE 780080, (1978).
19. Edwards, C.F., Siebers, D.L.,Hoskin, D.H., "A Study of the Autoignition Process of a Diesel Spray via High Speed Visualization", SAE 920108, 1992
20. Tao,F. , Chomiak, J., "Numerical Investigation of Reaction Zone Structure and Flame Liftoff of DI Diesel Sprays with Complex Chemistry ", SAE 2002-01-1114, (2002)
21. Curran, H.J., Gaffuri, P., Pitz, W.J., Westbrook,C.K., "A Comprehensive Modeling Study of n-Heptane Oxidation", Combust. Flame, Vol.114, p 149-177, (1998)
22. Curran, H.J., Gaffuri, P., Pitz, W.J., Westbrook,C.K., "A Comprehensive Modeling Study of iso-Octane Oxidation", Combust. Flame, Vol.129, p253-280, (2002)
23. Hu, H. and Keck, J.C., "Autoignition of diabatically compressed combustible gas mixtures", SAE 872110, (1987)
24. Griffiths, J.F., "Reduced Kinetic Models and Their Application to Practical Combustion Systems", Prog. Energy Combust. Sci. Vol.21, p.25-107, (1995)
25. Tao F., Golovitchev V. I., Chemiak J., "Self-Ignition and Early combustion Process of n-Heptane Sprays Under Diluted Air Conditions: Numerical Studies Based on Detailed chemistry", SAE 200-01-2931, 2000
26. Westbrook, C.K., Curran, H.J., Pitz, W.J., Griffiths,J.F., Mohamed,C. Wo, S.K., "The Effects of Pressure, Temperature, and Concentration on the Reactivity of Alkanes: Experiments and Modeling in a Rapid Compression Machine", Twenty-seventh Symposium (Int.) on Combustion, The Combustion Institute, p.371-378, (1998)
27. Hoskin D. H., Edwards C. F., Siebers D. L., "Ignition Delay Performance Versus Composition Of Model Fuels" SAE 920109, 1992.
28. Westbrook, C.K., Curran, H.J., Pitz, W.J., Griffiths,J.F., Mohamed,C., "Kinetic Modeling of Hydrocarbon Autoignition at Low and Intermediate

Temperatures in a Rapid Compression Machine", Proceedings of 3rd Workshop on Modeling of Chemical Reaction Systems, University of Heidelberg, 1996.

29. Warnatz J., Maas U., Dibble R. W., "Combustion" 3rd ed, Springer, 2001

30. Heywood, J.B., "Internal Combustion Engine Fundamentals", McGraw Hill, 1988.

31. "Test Methods for Rating Motor, Diesel and Aviation Fuels", ASTM Annual Book of Standards, Section 5, Vol. 05.04, 1948

32. "Test Methods for Rating Motor, Diesel and Aviation Fuels", ASTM Annual Book of Standards, Section 5, Vol. 05.04, 1974-74

33. "CFR F5 Cetane Method Diesel Fuel Rating Unit: Operation and Maintenance ", Waukesha Engine Division, Dresser Industries, Inc., 1995.

APPENDIX – NUMERICAL RESULTS

Diesel Fuel	ASTM D613 Cetane Number	Calculated Cetane Number
PRF	100.0	99.7
PRF	80.0	80.6
PRF	60.0	60.1
PRF	50.0	49.9
PRF	40.0	39.9
SRF	74.8	75.0
SRF	60.2	58.4
SRF	55.1	55.3
SRF	50.1	49.5
SRF	40.0	41.4
n-Heptane	56.0	56.0
US -2D	40.3	41.2
Sasol Turbodiesel^{TM}	56.4	57.3
Sasol SPD^{TM} diesel	75.4	75.1
* US 2D (28.8% aromatics)	46.5	47.0
* US 2D + 2EHN (0.25%)	52.5	51.5
* US 2D + DTBPO (0.25%)	49.7	50.1
* US 2D + Mix (0.125% 2EHN and 0.125% DTBPO)	49.9	50.9
* 3-Part Model (35% n-cetane, 35% 1-methyl naphthalene, 30% decalin)	46.6	45.1